THE ULTRAVIOLET-TO-NEAR-INFRARED SPECTRAL FLUX DISTRIBUTION OF FOUR BL LACERTAE¹

R. FALOMO,² A. TREVES,³ L. CHIAPPETTI,⁴ L. MARASCHI,⁵ E. PIAN,³ AND E. G. TANZI⁴
Received 1992 April 27; accepted 1992 June 17

ABSTRACT

We report on simultaneous UV, optical, and near-IR observations of four BL Lac objects. For three objects (PKS 0118-27, PKS 0301-24, and PKS 1538+14), we find that the spectral flux distribution from 8×10^{13} to 2.5×10^{15} Hz is well described by a single power law with spectral index $\alpha_{\nu} = 1.2$, $\alpha_{\nu} = 1.0$, and $\alpha_{\nu} = 1.3$, respectively. For H0323+02, after subtraction of the contribution due to the host galaxy, the spectral emission is again consistent with a single, flatter power law, $\alpha_{\nu} = 0.78$.

Subject headings: BL Lacertae objects: general — infrared: galaxies — ultraviolet: galaxies

1. INTRODUCTION

In general the overall spectral flux distribution (SFD) of BL Lac objects cannot be described by a single power law $(f_y \propto$ $v^{-\alpha}$). More complex forms, like broken power laws or a continuous steepening with increasing frequency (e.g., Landau et al. 1986; Cruz-Gonzales & Huchra 1984; Ballard et al. 1990; Brown et al. 1989) are used depending on the considered energy range. Spectral "breaks" are seen to occur between near-IR and optical or between optical and UV frequencies (e.g., Ghisellini et al. 1986). These observed "features" may be intrinsic to the nonthermal emission component or be due to other causes like reddening, a contribution from the host galaxy, and/or lack simultaneity among observations in different bands. The contribution of starlight from the galaxy, if nonnegligible with respect to the nonthermal emission, produces a steepening of the energy distribution in the optical and a flattening in the near-IR, while reddening introduces a steepening of the continuum at optical-UV frequencies. For instance, the spectral break observed in some objects between near-IR and optical is completely removed when proper reddening corrections are applied (e.g., Tanzi et al. 1989).

The nonthermal emission is usually interpreted as due to the synchrotron or synchrotron self-Compton processes. A detailed study of the spectral shape of the nonthermal component is clearly important in order to understand the physics of the emission region. In fact the observed "features" (as spectral breaks) if intrinsic to the emission may be associated to energy losses of the relativistic electrons.

We report here on quasi-simultaneous (within days) UV, optical, and near-IR observations of four BL Lac objects obtained in the course of our systematic multifrequency study of BL Lac objects (see, e.g., Tanzi et al. 1986; Falomo et al. 1988, 1989; Treves et al. 1989; Falomo & Treves 1990). For the three objects PKS 0118-27, PKS 0301-24, and PKS 1538+14, the UV observations are the first obtained thus far,

while for H0323+02, the UV spectrum is of higher quality than reported before.

2. TARGET OBJECTS

Three of the objects are bright, compact (flat-spectrum) radio sources identified as BL Lac objects (variable, polarized, featureless continuum), while the fourth one derives from the HEAO 1 X-ray survey.

2.1. PKS 0118-27

The optical magnitude ranges between $m_V=15.5$ and $m_V=17.0$ (Condon, Hicks, & Jauncey 1977; Thompson, Djorgovski, & De Carvalho 1990). The polarization has been measured by Impey & Tapia (1988, 1990) who report the value of 17.4%. IR optical photometry is given by Adam (1985), Tanzi et al. (1989), Allen, Ward, & Hyland (1982), Ballard et al. (1990), and Mead et al. (1990), who also observed a high and constant polarization. The X-ray flux observed by the Einstein satellite is 0.14 μ Jy at 1 keV (Ledden & O'Dell 1985). An absorption redshift z=0.559 was recently determined by Falomo (1991) from an intervening absorption feature attributed to the Mg II doublet.

2.2. PKS 0301 - 24

The optical magnitude ranges between 16.0 and 17.0 (Condon et al. 1977; Pica et al. 1980, 1988). Optical polarimetry by Impey & Tapia (1988, 1990) gave an average polarization of 10.6%. Near-IR observations were gathered by Allen et al. (1982), Wright, Ables, & Allen (1983), and Bersanelli et al. (1992). Thus far there is no X-ray detection, nor a redshift estimate.

2.3. PKS 1538 + 14

The optical identification ($m_V = 15.5$) and the spectroscopic confirmation are due to Wills & Wills (1974) who have been led to recognize it as a BL Lac object. Optical monitoring of the source by Kinman (1976) and Pica et al. (1988) evidenced a variability in the visual band of almost 2 mag (17.2 $\leq m_V \leq$ 19) and a weaker one in the blue band (Kidger 1988). The maximum optical polarization measured by Impey & Tapia (1990) was of 20%. The results of *IRAS* far-IR observations are reported by Impey & Neugebauer (1988) who also give the overall energy distribution which is peaked in the far-infrared. Observations in the millimetric spectral range are reported by Edelson (1987), and near-IR measurements have been performed by Allen et al. (1982) and Bersanelli et al. (1992). The

¹ Based on observations obtained at the European Southern Observatory, La Silla, Chile, and with the *International Ultraviolet Explorer* collected at the ESA Tracking Station at Villafranca.

² Osservatorio Astronomico di Padova, v. Osservatorio 5, 35122, Padova, Italy.

³ Scuola Internazionale Superiore di Studi Avanzati, Strada Costiera 11, 34014 Trieste, Italy.

⁴ Istituto di Fisica Cosmica, CNR, via Bassini 15, 20133 Milano, Italy.

⁵ Dipartimento di Fisica Universitá di Genova, Italy.

X-ray flux detected by Einstein is 0.15 µJy at 1 keV (Ledden & O'Dell 1985). The redshift z = 0.605 is reported by Stickel et al. (1992).

2.4. H0323 + 02

The flaring X-ray source H0323+02 was independently noted by Doxsey et al. (1981) and Piccinotti et al. (1982) because of its dramatic variability and is well studied at all frequencies (Feigelson et al. 1986, and references therein). The redshift z = 0.147 has been measured by Filippenko et al. (1986). The near-infrared flux emission has been studied by Ballard et al. (1990). The visual magnitude ranges from 15.5 to 17.5 (Doxsey et al. 1983; Feigelson et al. 1986; Pica et al. 1988) with short-term fluctuations.

The X-ray flux in the energy range 2–10 keV varied by about a factor of 3 between $\simeq 1 \mu Jy$ and 3 μJy with an occasional flare up to 10 μ Jy during a 6 month period (Doxsey et al. 1983), whereas the Einstein IPC data exhibited a 60 s dip of a factor of ~11 at X-ray energies greater than 0.6 keV but not at 0.25 keV. The data following the 60 s dip showed that the X-ray emission at 1 keV varied smoothly between 4.8 and 6.4 μ Jy. Ginga observations by Ohashi (1989) in the range 2-30 keV yielded a dramatic variation of the flux in 5 hr from 1.1 μ Jy to $0.4 \mu Jy$.

3. OBSERVATIONS

3.1. Ultraviolet Spectra

UV observations (see Table 1 for a journal of observations) were obtained using both the Short Wavelength Primary (SWP; range: 1200-1950 Å) and the Long Wavelength Primary (LWP; range: 2000-3200 Å) cameras on-board the International Ultraviolet Explorer (IUE). The sources were centered in the blind offset mode in the large aperture (10" × 20" oval) at coordinates measured on a blue POSS paper copy or on ESO plates. IUE line-by-line images have been calibrated in flux using curves provided by Bohlin &

Holm (1980) for the SWP camera and Cassatella, Lloyd, & Gonzales (1989) for the LWP camera. Net spectra have been extracted using an implementation of the Gaussian extraction procedure GEX (Urry & Reichert 1988) developed by one of us (L. C.) and running within the MIDAS interactive analysis system produced at ESO.

The spectrum of PKS 1538+14 was at the limit of detectability, but still clearly visible in the line-by-line spectrum. For this case only the extraction criteria of Urry & Reichert have been relaxed: the default procedure first makes a fit of the background and computes the rms of the residuals around this fit in the region where signal is expected, then proceeds to signal extraction only if the average signal is >rms/2. In our case we have observed this constraint to be >rms/3 to give evidence to the very faint signal.

Figure 1 shows the extracted UV spectra of the four objects. For the purpose of fitting, the flux data were binned in wavelength intervals of 50 Å or 100 Å, after some spectral regions, heavily affected by camera artifacts and cosmic-ray hits, had been excluded. The associated errors are the standard deviations in the considered wavelength intervals divided by $(N/3)^{1/2}$, where N is the number of pixels contained in each wavelength interval. This follows from the finding of a correlation length of ≈ 3 pixels in the cameras response, which roughly corresponds to their resolution (see Edelson et al. 1992 and Kinney, Bohlin, & Neill 1991). The UV spectrum of each object (jointly in LWP and SWP cameras when observations from both were available) was fitted by a single power law $F_{\lambda} \propto \lambda^{-\alpha}$ (see Fig. 1). The interval of confidence at the 90% level associated to the spectral index has been evaluated after Avni (1976) and Lampton, Margon, & Bowyer (1976). Spectral indices are reported in the legend of Figure 1.

Besides these UV spectra, we retrieve from *IUE* archive two previous observations of H0323+02 obtained in 1984 and 1988. These spectra, processed using the same procedure described above, are reported in Figure 2.

TABLE 1 JOURNAL OF OBSERVATIONS

Date	Instrumentation	Magnitude/Flux	
	PKS 0118-27		
1989 Aug 10.3	ESO 1.5 + BC + CCD	V = 16.1	
1989 Aug 9.6	ESO 2.2 + IR phot IUE + LWP	K = 12.5 $F_{\lambda}(2500 \text{ Å})^{a} = 0.23 \pm 0.02$	
PKS 0301 – 24			
1989 Aug 7.4	ESO 1.5 + BC + CCD ESO 2.2 + IR phot IUE + SWP IUE + LWP	$V = 16.2 K = 12.9 F_{\lambda}(1500 \text{ Å})^{a} = 0.32 \pm 0.03 F_{\lambda}(2500 \text{ Å})^{a} = 0.29 \pm 0.02$	
PKS 1538+14			
1988 Aug 4.3	ESO 1.5 + BC + CCD ESO 2.2 + IR phot IUE + LWP	V = 17.4 K = 13.4 $F_{\lambda}(2700 \text{ Å})^{a} = 0.06 \pm 0.01$	
H0323+02			
1989 Aug 11.3 1989 Aug 11.1 1989 Aug 10.6 1989 Aug 8.8	ESO 1.5 + BC + CCD ESO 2.2 + IR phot IUE + SWP IUE + LWP	$V = 16.7$ $K = 13.5$ $F_{\lambda}(1500 \text{ Å})^{a} = 0.19 \pm 0.02$ $F_{\lambda}(2500 \text{ Å})^{a} = 0.12 \pm 0.02$	

^a Units: 10⁻¹⁴ ergs cm⁻² s⁻¹ Å⁻¹ (see also text).

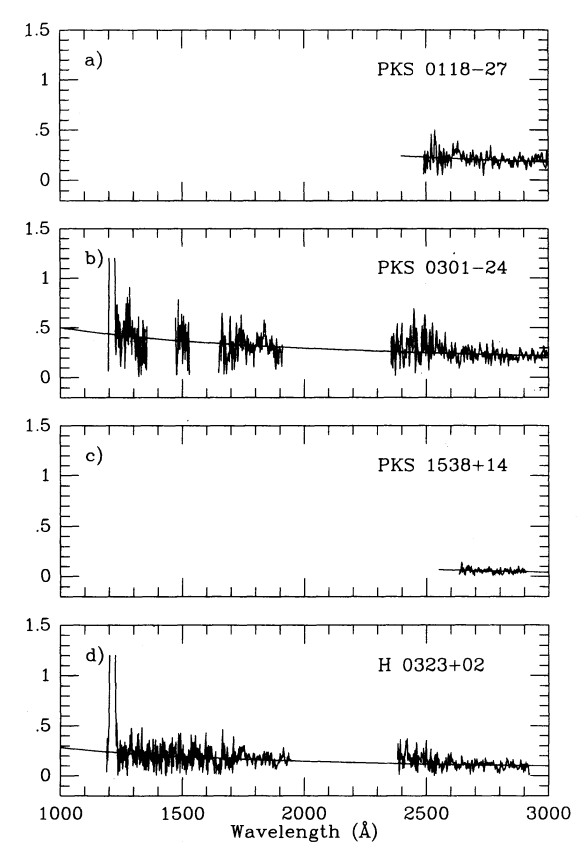


FIG. 1.—IUE extracted spectra of four BL Lac objects. (a) PKS 0118 – 27: $\alpha_{\lambda} = 1.31$, [-0.03, 2.57]; (b) PKS 0301 – 24: $\alpha_{\lambda} = 0.76$, [0.65, 0.88]; (c) PKS 1538 + 14: $\alpha_{\lambda} = 3.0$, [-1.5, 6.3]; (d) H0323 + 02: $\alpha_{\lambda} = 0.96$, [0.80, 1.11]. The spectral index α_{λ} is given with the error interval at the 90% confidence level in square brackets. The fitting power-law curve is superposed to each spectrum.

3.2. Optical Spectrophotometry

Optical spectrophotometry of the sources was obtained at the European Southern Observatory (ESO) 1.5 m telescope equipped with a Boller & Chivens spectrograph and CCD detector. Spectra were taken at a resolution of ≈ 15 Å (FWHM) through a long slit of 8" width. Standard reduction procedures were applied to obtain flux calibrated spectra. From repeated observations of standard stars (Stone 1977; Baldwin & Stone 1984) during each night, we derive a photometric accuracy better than 10%. To increase the signal-tonoise ratio, we obtained fluxes at intervals spaced of ~ 100 Å binning the spectra over bands of 100 Å.

3.3. Near-IR Photometry

J, H, K, and L photometry was obtained (see Table 1) at the ESO 2.2 m telescope (+ InSb photometer). A 15" circular aperture with chopper throw of 20" in the E-W direction was used. Statistical 1 σ errors are less than 0.1 mag in all bands. Conversion to flux units is made according to the zero-magnitude fluxes given in Bersanelli, Bouchet, & Falomo (1991).

4. OVERALL SPECTRA

A composite spectral flux distribution (SFD) was constructed for each object from quasi-simultaneous IR, optical, and UV observations. Errors in the UV were computed combining the statistical errors of each band (see previous section)

with a 10% systematic error. Data were corrected for interstellar reddening using A_V as deduced from the hydrogen column density (Stark et al. 1984) and assuming $N_H/E_{B-V}=5.8\times10^{21}$ (Bohlin, Savage, & Drake 1978). The interstellar extinction curve of Savage & Mathis (1979) for the optical–UV region and its extension to the IR by Whittet (1988) were used. The adopted values of A_V are given in the captions of Figures 3, 4, 5, and 6.

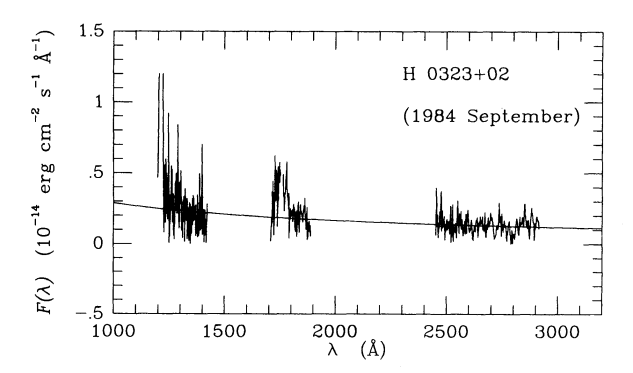
4.1. PKS 0118-27

The spectral flux distribution of PKS 0118-27 is reported in Figure 3. We find that a single power law of $\alpha_{\nu}=1.17\pm0.03$ is a good representation of the nonthermal emission from 8×10^{13} to 1.2×10^{15} Hz. There is no spectral signature in the SFD of the presence of a host galaxy.

4.2. PKS 0301 - 24

The overall spectral flux distribution of PKS 0301-24 from 1.2×10^{14} to 2.4×10^{15} Hz (see Fig. 4) can be described by a single power law of index $\alpha=1.01\pm0.03$ ($\chi^2_{\nu}\sim 1.9$). Although the data appear to be consistent with a single power-law model there are some deviations which could be real.

The near-IR-to-optical region exhibits a small curvature. Spectral indices in the optical and near-IR regions indicate that some curvature (break?) may be present at 5×10^{14} Hz ($\alpha_{\rm opt} = 1.17 \pm 0.04$; $\alpha_{\rm IR} = 0.83 \pm 0.22$). This could arise from the thermal contribution due to the host galaxy. To test this hypothesis we decomposed the spectrum into a power law plus an elliptical galaxy (assuming z = 0.2). We find the data are well fitted ($\chi^2_{\nu} \sim 0.9$) by the model with $\alpha_{\nu} = 0.84$ and a galaxy



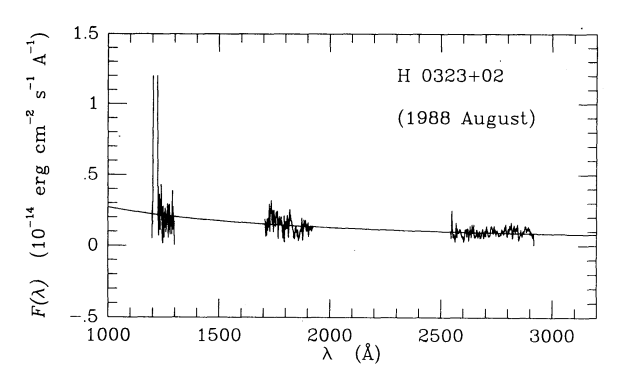


Fig. 2.—IUE extracted spectra of H0323+02 obtained from IUE archive. (a) SWP 24010 (exposure = 26,400 s) + LWP 4259 (exposure = 12,000 s) α_{λ} = 0.80, [0.57, 1.01]; (b) SWP 34098 (exposure = 30,000 s) + LWP 13873 (exposure = 11,040 s) α_{λ} = 1.08, [0.87, 1.28].

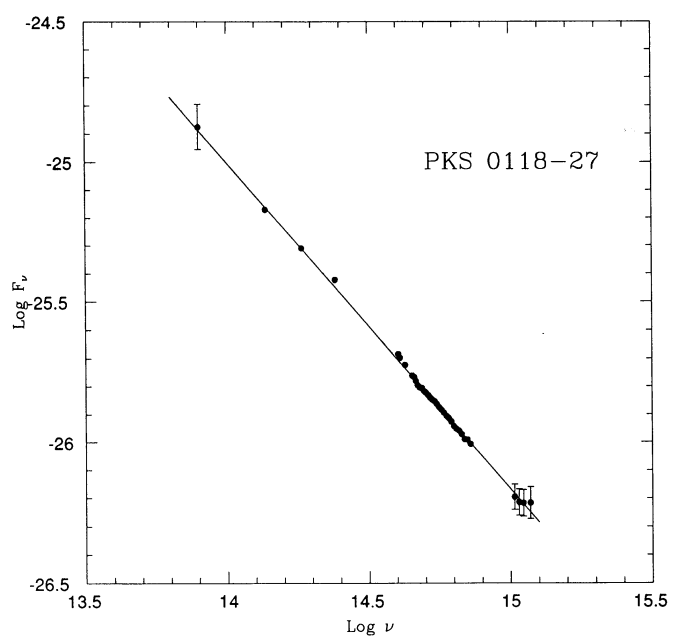


Fig. 3.—Spectral flux distribution of PKS 0118-27. Data have been dereddened with $A_V=0.1$. Only errors larger than 5% are plotted. Solid line represents the fitted power law of $\alpha=1.17$.

contributing 10% of total flux at 5500 Å. This corresponds to a galaxy of $M_V \sim -22$.

4.3. PKS 1538+14

This is the faintest source among those observed, and in fact it is at the limit of detectability with *IUE*. In the observed spectral range $(1.2 \times 10^{14} \text{ to } 1.2 \times 10^{15} \text{ Hz}$, the dereddened SFD (see Fig. 5) is consistent with a simple power-law model of $\alpha = 1.33 \pm 0.08$ ($\chi^2_{\nu} \sim 0.2$). We note, however, that a fit to the

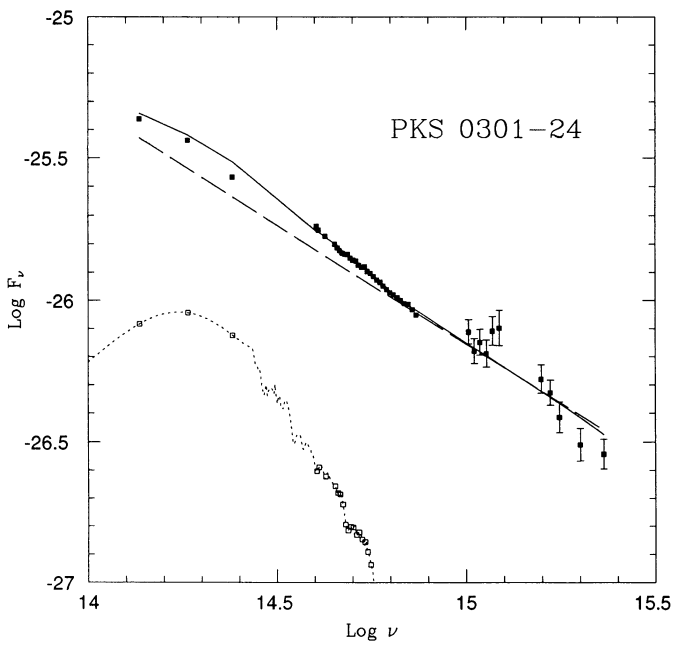


FIG. 4.—Spectral flux distribution of PKS 0301-24. Data have been dereddened with $A_V = 0.1$. Only errors larger than 5% are plotted. Solid line is the composition of a power law (dashed line) of $\alpha = 0.84$ plus an elliptical galaxy (dotted line) contributing to 10% of total flux at 5500 Å.

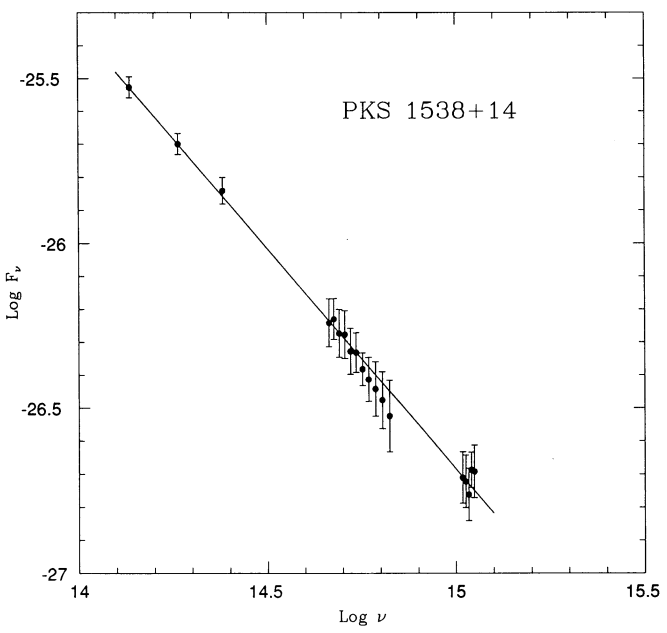


Fig. 5.—Spectral flux distribution of PKS 1538+14. Data have been dereddened with $A_V = 0.1$. Only errors larger than 5% are plotted. Solid line represents the fitted power law of $\alpha = 1.33$.

optical spectrum alone gives a significant steeper spectral index ($\alpha \sim 1.8$). This steeper value was repeatedly observed also at different other epochs (Falomo et al. 1992).

4.4. H0323 + 02

The X-ray-selected BL Lac object H0323+02 (Doxsey et al. 1983) is known to reside in a giant elliptical galaxy of $M_V \sim$

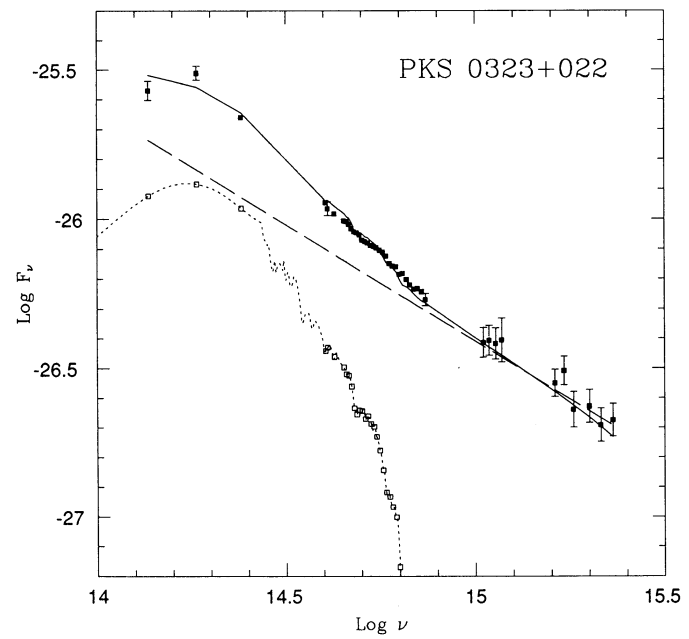


Fig. 6.—The near-IR-to-UV spectral flux distribution of H0323+02 in the 100 Å rebinning (filled squares) is decomposed into a power law (dashed line) with $\alpha_v = 0.65$ plus a standard elliptical galaxy (dotted line) redshifted at z = 0.147. The open squares represent the standard elliptical after rebinning as the observed data points, and the solid line is the sum of the two components. All data are dereddened with $A_V = 0.2$. Only errors larger than 5% are plotted.

536 FALOMO ET AL.

-22 (Feigelson et al. 1986; Fillipenko et al. 1986) which contributes substantially to the observed flux in the near-IR and optical range. Our overall spectrum (see Fig. 6) shows in fact a clear signature of a stellar population which flattens the energy distribution in the near-IR with respect to the optical.

To study the nonthermal component, we decomposed the UV-optical-to-IR spectral flux distribution into a giant elliptical superposed onto a single power-law emission. We assumed the standard elliptical of Yee & Oke (1978) with the near-IR colors of Arimoto & Yoshii (1987) for the thermal component and a single power law $(f_{\nu} \propto \nu^{-\alpha})$ for the nonthermal source.

We found that the observations can be well fitted by the superposition of the (standard) elliptical galaxy, contributing 25% of the observed flux at 5500 Å, plus a flat nonthermal component of spectral index $\alpha_v = 0.78$. The absolute magnitude of the host galaxy as derived from the decomposition of the SFD is $M_V = -21.6$ assuming $H_0 = 50$; $q_0 = 0$. This decomposition is consistent with that performed by Filippenko et al. (1986) using only optical spectrum and indicates that the nonthermal component described by a flat power law extends from 2×10^{14} to 5×10^{15} Hz.

The source was observed with *IUE* at previous epochs (see Fig. 2 and Table 2). It is apparent that no significant variability in the intensity and spectral shape is present within the errors.

5. DISCUSSION AND CONCLUSIONS

We obtained quasi-simultaneous observations at various wavelengths for four BL Lac objects. This allows to study the broad-band continuum from IR to UV taking into account the reddening correction and the contribution from the host galaxy.

We found that in all cases observed the SFD is well accounted for either by a single power law $(f_{\nu} \propto \nu^{-\alpha})$ or by a power law plus an elliptical galaxy. The large polarization observed in the optical together with the continuity of the

TABLE 2
ARCHIVAL IUE OBSERVATIONS: H0323+02

Date	Instrumentation	Flux
1984 Sep 19.9	IUE + SWP	$F_{\lambda}(1500 \text{ Å})^{a} = 0.18 \pm 0.05$
1984 Sep 20.3	IUE + LWP	$F_{\lambda}(2600 \text{ Å})^{a} = 0.12 \pm 0.02$
1988 Aug 18.9	IUE + SWP	$F_{\lambda}(1700 \text{ Å})^{a} = 0.18 \pm 0.02$
1988 Aug 19.0	IUE + LWP	$F_{\lambda}(2500 \text{ Å})^{a} = 0.09 \pm 0.01$

^a Units: 10⁻¹⁴ ergs cm⁻² s⁻¹ Å⁻¹ (see also text).

spectral shape strongly suggests that in the entire IR-to-UV range the dominant emission mechanism is synchrotron radiation. There is no clear signature in the overall spectra observed of a steepening of the nonthermal continuum, indicating that energy losses of relativistic electrons would occur at higher frequencies than UV.

It may be noticeable that the slope for H0323 + 02, $\alpha_v = 0.78$, which is an X-ray-selected object is flatter than that of PKS 0118-27, PKS 0301-24, PKS 1538+14, which instead are radio selected. This agrees with our findings based on the examination of archival data of a collection of 33 *IUE*-observed BL Lac objects (Maraschi et al. 1986; Ghisellini et al. 1986) and confirmed by Bersanelli et al. (1992) for a large set of homogeneous IR measurements of BL Lac objects.

The power law which describes the nonthermal component in the IR-UV domain can be extrapolated to the X-ray band and compared with the observed flux. In the case of PKS 1538+14 and H0323+02, the extrapolation is consistent, within the uncertainty, with the Einstein fluxes at 1 keV. The expected flux for PKS 0118-27 is a factor ~ 5 higher than the observed one, which may be attributed to a steepening of the spectrum or to nonsimultaneous observations. We note that the optical UV observations were taken during a high state of the source. Finally, the extrapolated flux for PKS 0301-24 is $\sim 2.7 \,\mu$ Jy at 1 keV. Therefore the source should be successfully detected with the ROSAT satellite.

REFERENCES

Kidger, M. R. 1988, PASP, 100, 1248

Kinger, M. K. 1966, PASF, 100, 1246
Kinman, T. D. 1976, ApJ, 205, 1
Kinney, A., Bohlin, R., & Neill, J. 1991, PASP, 103, 694
Lampton, M., Margon, B., & Bowyer, S. 1976, ApJ, 208, 177
Landau, R., et al. 1986, ApJ, 308, 78
Ledden, J. E., & O'Dell, S. L. 1985, ApJ, 298, 630
Maraschi, L., Ghisellini, G., Tanzi, E. G., & Treves, A. 1986, ApJ, 310, 325
Mead, A. R. G., Ballard, K. R., Brand, P. W. J. L., Hough, J. H., Brindle, C., & Bailey, J. A. 1990, A&AS, 83, 183
Ohashi, T. 1989, in BL Lac Objects, ed. L. Maraschi, T. Maccacaro, & M.-H.
Ulrich (Berlin: Springer-Verlag), 96
Pica, A. J., Pollock, J. T., Smith, A. G., Leacock, R. J., Edwards, P. L., & Scott,
R. L. 1980, AJ, 85, 1442
Pica, A. J., Smith, A. G., Webb, J. R., Leacock, R. J., Clements, S., & Gombola,
P. P. 1988, AJ, 96, 1215
Piccinotti, G., Mushotzky, R. F., Boldt, E. A., Holt, S. S., Marshall, F. E.,
Serlemitsos, P. J., & Shafer, R. A. 1982, AJ, 253, 485
Savage, B. D., & Mathis, J. S. 1979, ARA&A, 17, 73
Stark, A. A., Heiles, C., Bally, J., & Linde, R. 1984, Bell Labs., privately distributed tape
Stickel, M., Padovani, P., Urry, C. M., Fried, J. W., & Kühr, H. 1991, ApJ, 374, 431
Stone, R. P. S. 1977, ApJ, 218, 767
Tanzi, E. G., Falomo, R., Bouchet, P., Bersanelli, M., Maraschi, L., & Treves,
A. 1989, in BL Lac Objects, ed. L. Maraschi, T. Maccacaro, & M.-H. Ulrich
(Berlin: Springer-Verlag), 171
Thompson, D. J., Djorgovski, S., & De Carvalho, R. 1990, PASP, 102, 1235
Treves, A., Morini, M., Chiappetti, L., Fabian, A., Falomo, R., Maccagni, D.,
Maraschi, L., Tanzi, E. G., & Tagliaferri, G. 1989, ApJ, 341, 733
Urry, C. M., & Reichert, G. 1988, IUE NASA Newsletter, 34, 96
Wills, D., & Wills, B. J. 1974, ApJ, 190, 271
Whittet, D. C. B. 1988, in Dust in the Universe, ed. M. E. Bailey & D. A.
Williams (Cambridge: Cambridge Univ. Press), 25
Wright, A. E., Ables, J. G., & Allen, D. A. 1983, MNRAS, 205, 793
Yee, H. K. C., & Oke, J. B. 1978, ApJ, 226, 769